HHS Public Access

Author manuscript

Cell Rep. Author manuscript; available in PMC 2017 September 01.

Published in final edited form as:

Cell Rep. 2017 June 27; 19(13): 2657–2664. doi:10.1016/j.celrep.2017.05.092.

PP6 Disruption Synergizes with Oncogenic Ras to Promote JNK-dependent Tumor Growth and Invasion

Xianjue Ma[1,4], **Jin-Yu (Jim) Lu**[1,3,4], **Yongli Dong**[1], **Daming Li**[1], **Juan N. Malagon**[1], and **Tian Xu**[1,2,5]

[1]Howard Hughes Medical Institute, Department of Genetics, Yale University School of Medicine, 295 Congress Avenue, New Haven, CT 06519, USA

[2]State Key Laboratory of Genetic Engineering and National Center for International Research, Fudan-Yale Biomedical Research Center, Institute of Developmental Biology and Molecular Medicine, School of Life Sciences, Fudan University, Shanghai 200433, China

Summary

RAS genes are frequently mutated in cancers, yet an effective treatment has not been developed. This is partly due to an incomplete understanding of signaling within Ras-related tumors. To address this, we performed a genetic screen in *Drosophila*, aiming to find mutations that cooperate with oncogenic Ras (Ras^{V12}) to induce tumor overgrowth and invasion. We identified *fiery mountain* (*fmt*), a regulatory subunit of the protein phosphatase 6 (PP6) complex, as a tumor suppressor that synergizes with Ras^{V12} to drive JNK-dependent tumor growth and invasiveness. We show that Fmt negatively regulates JNK upstream of dTAK1. We further demonstrate that disruption of *PpV*, the catalytic subunit of PP6, mimics *fmt* loss of function induced tumorigenesis. Finally, Fmt synergizes with PpV to inhibit JNK-dependent tumor progression. Our data here further highlight the power of *Drosophila* as a model system to unravel molecular mechanisms that may be relevant to human cancer biology.

Graphical abstract

Correspondence: tian.xu@yale.edu.

[3]Present Address: Yale-Waterbury Internal Medicine Residency Program, 64 Robbins Street, Waterbury CT 06708, USA.

[4]These authors contribute equally

[5]Lead Contact

Author Contributions

X.M., J-Y L. and T.X. conceived the study. X.M. and J-Y L. performed experiments and analyzed data. Y.D. and D.L. assisted in immunofluorescence staining. J.M. assisted with model drawing. X.M., and T.X. wrote the manuscript.

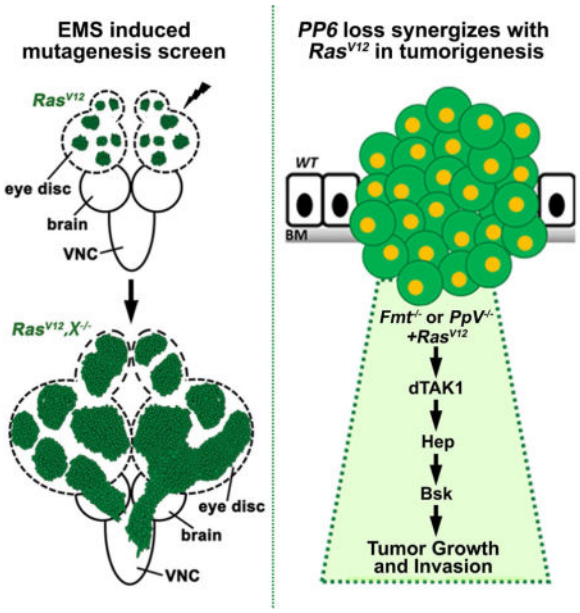

Keywords

Ras; Fmt; PpV; JNK; tumorigenesis; *Drosophila*

Introduction

The *RAS* family genes (*HRAS*, *NRAS* and *KRAS*) are the most frequently mutated genes in cancer (Ryan et al., 2015; Vogelstein et al., 2013). The discovery of *RAS* in 1982 has catapulted the pursuit of an anti-*RAS* therapy to the forefront of pharmaceutical cancer research (Cox et al., 2014; Der et al., 1982; Ryan et al., 2015; Samatar and Poulikakos, 2014). However, despite several decades of concentrated effort and breakthroughs, successful therapeutic methods targeting RAS-related cancers remain to be developed (Cox et al., 2014; Ryan et al., 2015; Stephen et al., 2014), largely due to the lack of a systematic understanding of the complex signaling crosstalk within *RAS* tumors.

A large scale screenable tool would be beneficial to comprehensively dissect genetic alternations in the *RAS* tumors. Given conservation of cancer-related genes and signaling pathways between humans and *Drosophila* (Reiter et al., 2001), and taking into account the difficulty of systematically study the mechanisms of tumor progression in patients, *Drosophila* has been widely used as an *in vivo* model to study the genetic mechanism and signaling pathways that regulate various aspects of cancer biology, using relative easy genetic manipulation (deletion/overexpression) and large scale screens (Brumby et al., 2011; Chi et al., 2010; Khoo et al., 2013; Pastor-Pareja and Xu, 2013). Indeed, over the past decade, numerous tumor growth and invasion models have been established in larvae and adult flies (Figueroa-Clarevega and Bilder, 2015; Gonzalez, 2013; Kwon et al., 2015; Pagliarini and Xu, 2003; Pastor-Pareja and Xu, 2013; Rudrapatna et al., 2012; Willoughby et al., 2013). In particular, oncogenic Ras (Ras^{V12}) has been shown to cooperate with mutants that disrupt cell polarity to drive tumor growth and invasion in fly (Brumby and Richardson,

2003; Pagliarini and Xu, 2003). The existence of these models and tools makes *Drosophila* a fantastic *in vivo* model to dissect Ras^{V12} mediated tumorigenesis.

Here we performed a large scale EMS-induced genetic screen, aiming to unearth tumor suppressors that can synergistically enhance Ras^{V12} induced tumor growth. We identify Fmt as a tumor suppressor that negatively regulates JNK signaling. The combination of Ras^{V12} with loss of *fmt* induces dramatic tumor overgrowth and invasion behavior upstream of dTAK1. We further show that PpV, the homolog of mammalian catalytic subunit of the protein phosphatase 6 (PP6), also functions as a tumor suppressor and synergizes with Fmt *in vivo* to inhibit JNK mediated tumorigenesis. These findings not only shed light on the molecular mechanism of PP6-mediated tumorigenesis, but also provide a potential target for drug development for oncogenic Ras related cancer.

Results

Fmt encodes a novel tumor suppressor that synergizes with Ras^{V12} to drive tumorigenesis and invasion

Based on the observation that oncogenic Ras (Ras^{V12}) alone can only induce mild benign tumors (Brumby and Richardson, 2003; Pagliarini and Xu, 2003), we utilized the *ey*-FLP based MARCM (mosaic analysis with repressible cell marker) technique to conduct an EMS-induced forward genetic screen on *Drosophila* chromosome 3L, aiming to identify novel tumor suppressors that can synergize with Ras^{V12} to drive dramatic tumor overgrowth and invasion in the developing eye (Figure 1A). We screened more than 20,500 mutagenized chromosomes and successfully identified over 200 mutations that accelerate the growth of Ras^{V12} tumors (details of the screen will be published elsewhere). Among the candidates, we isolated a recessive-lethal complementation group consisting of four alleles that exhibited invasive tumor overgrowth (Figures S1A–B). Subsequent deficiency mapping revealed that each one disrupted the gene *CG10289*, which encodes a highly conserved 991 amino acid protein, homologous to human PPP6R1, PPP6R2 and PPP6R3 (protein phosphatase 6 regulatory subunits) (Figure S1C). We named *CG10289 fiery mountain* (*fmt*), after a famous Chinese mountain in Xinjiang province.

7 days after egg laying (AEL), the $Ras^{V12}/fmt^{-/-}$ clones hyper-proliferate extensively, compared with Ras^{V12} expression alone (Figures 1 B and S1D), whereas no GFP positive cells were observed in the ventral nerve cord (VNC) (Figures 1B′ and S1D′), a well-known organ for tumor cell invasion observation in *Drosophila* (Igaki et al., 2006; Pagliarini and Xu, 2003). At 11 days AEL, with continuous tumor progression, 45% of $Ras^{V12}/fmt^{-/-}$ animals displayed invasive behavior (Figures 1C and C′), along with intensive MMP1 activation, a protein essential for basement membrane degradation and EMT progression (Srivastava et al., 2007; Uhlirova and Bohmann, 2006), in both primary tumor and invasive leading edge (Figures 1D″, E″ and S1M–P). In agreement with this, we also observed dramatically increased autonomous mitosis and enhanced epithelial integrity in $Ras^{V12}/fmt^{-/-}$ tumors (Figures S1E–L). Conversely, we did not detect significant changes in apoptosis (Figures S1Q–S). Taken together, these findings identify Fmt as a novel tumor suppressor that can synergize with Ras^{V12} to induce tumor growth and invasion.

Fmt negatively regulates JNK signaling

MMP1 serves as a transcriptional target of JNK signaling in tumor cell invasion (Srivastava et al., 2007; Uhlirova and Bohmann, 2006), suggesting that $Ras^{V12}/fmt^{-/-}$ may promote tumorigenesis via JNK activation. Consistent with this prediction, a canonical JNK pathway target, *puc*, was strongly activated in $Ras^{V12}/fmt^{-/-}$ tumors (Figures S2A–B). Interestingly, we found that depletion of *fmt* alone was sufficient to induce mild JNK activation autonomously (Figures 2B′–C′), indicating that Fmt is a negative regulator of the JNK pathway. To further test this, we first asked whether Fmt is essential for the small eye phenotype caused by ectopic expression of Eiger (Egr), the sole TNF-α ligand which activates JNK in *Drosophila* (Igaki et al., 2002; Moreno et al., 2002). We found that *GMR*>Egr induced small eye phenotype was significantly enhanced by reducing *fmt* expression, while expression of *fmt-IR* itself caused no obvious phenotype (Figures 2D–G). We have previously shown that *scribbled* (*scirb*) deficient cells undergo JNK-dependent elimination (Igaki et al., 2009), so we tested whether Fmt is required for this process. As expected, the survival defect of *scrib* mutant clones was significantly rescued by ectopic expression of Fmt (Figures 2H–K). Furthermore, consistent with our hypothesis, we found that inhibition of JNK activity by expression of a dominant negative form of *Drosophila* JNK homolog Basket (Bsk^{DN}) completely abolished $Ras^{V12}/fmt^{-/-}$ induced tumor growth, invasive phenotype and JNK activation (Figures 2L, M and S2C–G). Together, these data indicate that Fmt negatively regulates JNK signaling *in vivo*.

To further dissect the mechanism of how Fmt modulates JNK signaling, we performed epistasis analysis between Fmt and known JNK pathway components in the developing wing. Similar to elevated JNK activation (Ma et al., 2015; Ma et al., 2013), expression of *fmt-IR* under *patched* (*ptc*) promoter resulted in partial or complete loss of the anterior cross vein (Figures 2N and S2H–I), which can be significantly suppressed by co-expression of the JNK phosphatase Puckered (Puc), expression of Bsk^{DN}, reducing activity of JNK kinase Hemipterous (Hep), or inhibition of dTAK1, whereas it remained unaffected by blocking dTRAF2 or Msn (Figure 2O). In agreement with this genetic evidence, we found inhibition of dTAK1 activity also significantly impeded $Ras^{V12}/fmt^{-/-}$ induced tumor growth and completely suppressed the invasive behavior (Figures S2J–K). Together, these data demonstrate that Fmt negatively regulates JNK signaling upstream of dTAK1.

PpV depletion synergizes with Ras^{V12} to induce dTAK1-JNK dependent tumorigenesis

Fmt contains an evolutionarily conserved SAPS (SIT4 phosphatase-associated proteins) domain (Figure S1C), encoding a regulatory subunit, which interacts with another catalytic subunit (PPP6C, PpV in *Drosophila*) to form a functional PP6 holoenzyme (Douglas et al., 2010; Hosing et al., 2012). Interestingly, *PPP6C* has been recently recognized as a potential tumor suppressor, since it is significantly mutated in melanoma, although the underlying mechanism remains poorly understood (Hodis et al., 2012; Krauthammer et al., 2012). Paradoxically, studies in fly indicate that *PpV* depletion results in a growth defect (Friedman et al., 2011), suggesting a growth promoting role for PPP6C. To resolve this contradiction and clarify PpV's *in vivo* role during tumor progression, we generated a null allele of *PpV* that deletes its entire coding region by imprecise *P* element excision (Figure S3A). Similar to that of *fmt* disruption, we observed mild JNK activation in *PpV* mutant clones (Figures

3A–B). In line with this, we found loss of *PpV* significantly enhanced *GMR*>Egr induced small eye phenotype (Figures 3C–D and S3C–D), illustrating the role of PpV as a negative regulator of JNK signaling. More importantly, loss of *PpV* synergizes with Ras^{V12} to drive massive MMP1 activation, tumor overgrowth, invasion and metastasis into other organs (Figures 3E–F, I–J and S3B, E–F). Consistent with the epistasis analysis of Fmt, we found $PpV^{-/-}/Ras^{V12}$ induced tumor progression was completely or dramatically impeded blocking JNK activity (Figures 3G, H, K and S3G), or inhibition of dTAK1 (Figure S3H). Collectively, these data indicate that PpV encodes a tumor suppressor that collaborates with Ras^{V12} to drive JNK-dependent tumor growth and invasion through dTAK1.

Fmt synergizes with PpV *in vivo*

To gain further insights into the *in vivo* function(s) of Fmt and PpV in regulating the JNK pathway, we knocked down or ectopically expressed Fmt and PpV in different tissues. We found that simultaneous reduction of Fmt and PpV under *nubbin* (*nub*) promoter synergistically reduced wing size, phenocopying elevated JNK activity (Lee et al., 2006), an effect that is not observed under expression of *Fmt-IR* or *PpV-IR* alone (Figures 4H–L). Similarly, removing one copy each of *fmt* and *PpV* synergistically enhance *GMR*>Eiger eye phenotype and result in a complete loss of the eye tissue (Figures 4A–D). Conversely, ectopic expression of Fmt and PpV suppress *GMR*>Egr-induced small eye in a synergistic way (Figures 4E–G). We previously showed that the combination of cell polarity disruption and Ras^{V12} activation induces JNK dependent tumor growth and invasive behavior (Igaki et al., 2006; Pagliarini and Xu, 2003). In accordance with the observation that Fmt and PpV negatively regulate the JNK pathway (Figures 2 and 3), we found that over-expression of Fmt or PpV alone is sufficient to partially or completely suppress the tumor invasion and rescued the $lgl^{-/-}/Ras^{V12}$ bearing animals to pupae stage (Figures 4F–H, F″–H″), while the tumor size remained relatively unaffected (Figures 4F′–H′). Strikingly, when Fmt and PpV were co-expressed, $lgl^{-/-}/Ras^{V12}$ induced tumor growth, invasion and MMP1 activation were dramatically suppressed (Figures 4I–I″ and S4C–D), indicating a synergistic role of Fmt and PpV in tumor inhibition. It is noteworthy that residual MMP1 activation still detected, in line with our observation that co-expression of Fmt and PpV cannot fully suppress *GMR*>Egr small eye phenotype (Figure 4G). As tumor progression is frequently accompanied by apoptosis (Menendez et al., 2010; Vidal et al., 2006), to test if Fmt and PpV block tumorigenesis by inducing apoptosis, we monitored caspase 3 activation and found that co-expression of Fmt and PpV did not induce massive apoptosis in $Ras^{V12}/lgl^{-/-}$ clones (Figure S4), suggesting that the tumor suppressing role of Fmt and PpV is uncoupled from apoptosis. Finally, we found that co-expression of Ras^{V12} and *PpV-IR* induced mild tumor overgrowth and MMP1 activation was dramatically enhanced by deleting one copy of *fmt* (Figures S4E–G), further confirming the *in vivo* synergistic effect between Fmt and PpV in tumorigenesis.

Discussion

In this study, we have conducted an unbiased, EMS-based forward genetic screen and identified Fmt and PpV as tumor suppressors that cooperate with Ras^{V12} to induce massive tumor overgrowth and invasion. Our genetic epistasis analysis establish Fmt and PpV as

essential negative regulators of the JNK pathway, acting upstream of dTAK1 (Figure 4J). Moreover, we found that Fmt/PpV synergistically inhibits JNK-mediated tumorigenesis *in vivo*. Interestingly, the human homolog of PpV, the catalytic subunit of the PP6 holoenzyme (PPP6C), was recently identified as a driver mutation during melanoma progression. Approximately 10% of patients were found to harbor *PPP6C* somatic mutations (Hodis et al., 2012; Krauthammer et al., 2012), and surprisingly, all of them had *BRAF* or *RAS* mutations as well (Krauthammer et al., 2012). Apart from the known roles of PP6 in regulating cell cycle and mitosis (Stefansson and Brautigan, 2007; Zeng et al., 2010), little is understood about the genetic mechanism by which it modulates tumor growth. Here, we have uncovered the underlying mechanism of $PP6^{-/-}/Ras^{V12}$ induced tumor overgrowth, and identified dTAK1-JNK signaling as the essential molecular link, which also further demonstrates the value of the *Drosophila* model system for gaining insight into human cancer biology. Interestingly, human PP6 is known to directly bind and dephosphorylate TAK1 at Thr-187 (Kajino et al., 2006), suggesting a conserved role of PP6-TAK1 module. Given the conservation of signaling pathways between *Drosophila* and humans, similar mechanisms could be involved in human $PP6\text{-}Ras^{V12}$ related cancer progression. Further investigation in mammal and human may provide potential therapeutic targets for cancer treatment, especially melanoma.

Experimental Procedures

Drosophila stocks and genetics

All crosses were raised on standard *Drosophila* media at 25°C unless otherwise indicated. Fluorescently labeled clones were produced in the eye discs as previously described (Pagliarini and Xu, 2003) using the following strains: *tub*-Gal80, FRT19A; *ey-Flp5*, *Act>y*$^{+}$>Gal4, *UAS*-GFP (19A tester); *ey-Flp1*; *tub*-Gal80, FRT40A; *Act>y*$^{+}$>Gal4, *UAS*-GFP (40A tester); *ey-Flp1*; *Act>y*$^{+}$>Gal4, *UAS*-GFP; *tub*-Gal80, FRT79E (79E tester); *eyFlp1*; *Act>y*$^{+}$>Gal4, *UAS*-GFP.S65T; FRT82B, *tub*-Gal80 (82B tester). Additional strains, including KG09672, *GMR*-Gal4, *ptc*-Gal4, *nub*-Gal4, *UAS*-GFP, *UAS-msn-IR, UAS-PpV* (#53770) were obtained from Bloomington *Drosophila* Stock Center; *UAS*-dTAK1^{DN}, *UAS-dTRAF2-IR* (Xue et al., 2007), *puc*^{E69}, *UAS*-Egr, *lgl*^{4}, *UAS-Ras*^{V12}, *UAS*-Puc (Ma et al., 2014), *UAS*-Bsk^{DN}, *UAS-hep-IR* (Ma et al., 2015), *scrib*^{1} (Igaki et al., 2009) were previously described. *UAS-PpV-IR* (V31690) and *UAS-Fmt-IR* (V16005) were obtained from the Vienna *Drosophila* RNAi Center; *UAS*-PpV^{HA} (F000874) was obtained from FlyORF.

PpV mutants were generated by imprecise excision of the the *P* element insertion line KG09672. Genomic DNA of isolated candidate mutants were isolated and analyzed by PCR. Sequence analysis indicated that the $PpV^{\Delta 1}$ allele deletes the entire coding region of *PpV*, suggesting that $PpV^{\Delta 1}$ is a null allele.

UAS-Fmt transgenic flies were generated by standard *P* element-mediated transformation. Two independent lines (on second and third chromosomes) were produced and examined for each transgene, and gene expression was verified by RT-PCR.

EMS mutagenesis and genetic screen

We focus on the left arm of chromosome 3, which covers around 20% of the fly genome. Male flies carrying a FRT79E (Sp/CyO-GFP; FRT79E) were starved for 8 hr and subsequently fed a 25 mM ethyl methanesulphonate (EMS) solution overnight at room temperature. The mutagenized males were mated to females of the genotype *UAS-Ras*^{V12}; *sb*/TM6B. Single F1 males of the genotype *UAS-Ras*^{V12}/CyO-GFP; *FRT79E/TM6B were crossed to Sp/CyO; sb/TM6B first and then crossed to a 79E tester line. The larvae are transparent and can be easily scored for overgrowth of GFP-labeled tumor caused by enhancer mutations.

Immunostaining

Third instar larvae eye-antennal discs were dissected in 1× PBS, fixed in freshly made 4% paraformaldehyde and stained as described previously (Ma et al., 2013), using mouse anti-MMP1 (1:200), mouse anti-β-Gal (1:1000, DSHB, Developmental Studies Hybridoma Bank), rabbit anti-phospho histone 3 (PH3) (1:200), rabbit anti-active Caspase 3 (1: 400) and Alexa Fluor®555 (1:100, Cell Signaling Technology). Secondary antibodies were anti-rabbit-Alexa (1:400), and anti-mouse-Cy3 (1:400, Thermo Fisher Scientific). Tumor growth and invasion images in Figureure 1 and 4 were taken with a Leica MZ FLIII fluorescence stereomicroscope with an Optronics Magnafire S99802 digital camera.

Statistical analysis

Clone and wing size were measured with Image J and Photoshop, respectively. Quantification of the data was presented in bar graphs created with Graphpad Prism 5. Data represents mean values + SD. We used a one-way ANOVA with Bonferroni correction for multiple comparisons to calculate statistical significance (**P<0.01; ***P<0.001).

Supplementary Material

Refer to Web version on PubMed Central for supplementary material.

Acknowledgments

We thank Bloomington and VDRC stock centers for providing fly stocks, C. Chabu, B. Dunn for discussion and comments, J. Kouptsova for critical reading of the manuscript. This research was supported by a NIH/NCI grant to T.X, T.X. is a Howard Hughes Medical Institute Investigator.

References

Brumby AM, Goulding KR, Schlosser T, Loi S, Galea R, Khoo P, Bolden JE, Aigaki T, Humbert PO, Richardson HE. Identification of novel Ras-cooperating oncogenes in Drosophila melanogaster: a RhoGEF/Rho-family/JNK pathway is a central driver of tumorigenesis. Genetics. 2011; 188:105–125. [PubMed: 21368274]

Brumby AM, Richardson HE. scribble mutants cooperate with oncogenic Ras or Notch to cause neoplastic overgrowth in Drosophila. The EMBO journal. 2003; 22:5769–5779. [PubMed: 14592975]

Chi C, Zhu H, Han M, Zhuang Y, Wu X, Xu T. Disruption of lysosome function promotes tumor growth and metastasis in Drosophila. The Journal of biological chemistry. 2010; 285:21817–21823. [PubMed: 20418542]

Cox AD, Fesik SW, Kimmelman AC, Luo J, Der CJ. Drugging the undruggable RAS: Mission possible? Nature reviews Drug discovery. 2014; 13:828–851. [PubMed: 25323927]

Der CJ, Krontiris TG, Cooper GM. Transforming genes of human bladder and lung carcinoma cell lines are homologous to the ras genes of Harvey and Kirsten sarcoma viruses. Proceedings of the National Academy of Sciences of the United States of America. 1982; 79:3637–3640. [PubMed: 6285355]

Douglas P, Zhong J, Ye R, Moorhead GB, Xu X, Lees-Miller SP. Protein phosphatase 6 interacts with the DNA-dependent protein kinase catalytic subunit and dephosphorylates gamma-H2AX. Molecular and cellular biology. 2010; 30:1368–1381. [PubMed: 20065038]

Figueroa-Clarevega A, Bilder D. Malignant Drosophila tumors interrupt insulin signaling to induce cachexia-like wasting. Developmental cell. 2015; 33:47–55. [PubMed: 25850672]

Friedman AA, Tucker G, Singh R, Yan D, Vinayagam A, Hu Y, Binari R, Hong P, Sun X, Porto M, et al. Proteomic and functional genomic landscape of receptor tyrosine kinase and ras to extracellular signal-regulated kinase signaling. Science signaling. 2011; 4:rs10. [PubMed: 22028469]

Gonzalez C. Drosophila melanogaster: a model and a tool to investigate malignancy and identify new therapeutics. Nat Rev Cancer. 2013; 13:172–183. [PubMed: 23388617]

Hodis E, Watson IR, Kryukov GV, Arold ST, Imielinski M, Theurillat JP, Nickerson E, Auclair D, Li L, Place C, et al. A landscape of driver mutations in melanoma. Cell. 2012; 150:251–263. [PubMed: 22817889]

Hosing AS, Valerie NC, Dziegielewski J, Brautigan DL, Larner JM. PP6 regulatory subunit R1 is bidentate anchor for targeting protein phosphatase-6 to DNA-dependent protein kinase. The Journal of biological chemistry. 2012; 287:9230–9239. [PubMed: 22298787]

Igaki T, Kanda H, Yamamoto-Goto Y, Kanuka H, Kuranaga E, Aigaki T, Miura M. Eiger, a TNF superfamily ligand that triggers the Drosophila JNK pathway. The EMBO journal. 2002; 21:3009–3018. [PubMed: 12065414]

Igaki T, Pagliarini RA, Xu T. Loss of cell polarity drives tumor growth and invasion through JNK activation in Drosophila. Current biology: CB. 2006; 16:1139–1146. [PubMed: 16753569]

Igaki T, Pastor-Pareja JC, Aonuma H, Miura M, Xu T. Intrinsic tumor suppression and epithelial maintenance by endocytic activation of Eiger/TNF signaling in Drosophila. Developmental cell. 2009; 16:458–465. [PubMed: 19289090]

Kajino T, Ren H, Iemura S, Natsume T, Stefansson B, Brautigan DL, Matsumoto K, Ninomiya-Tsuji J. Protein phosphatase 6 down-regulates TAK1 kinase activation in the IL-1 signaling pathway. The Journal of biological chemistry. 2006; 281:39891–39896. [PubMed: 17079228]

Khoo P, Allan K, Willoughby L, Brumby AM, Richardson HE. In Drosophila, RhoGEF2 cooperates with activated Ras in tumorigenesis through a pathway involving Rho1-Rok-Myosin-II and JNK signalling. Disease models & mechanisms. 2013; 6:661–678. [PubMed: 23324326]

Krauthammer M, Kong Y, Ha BH, Evans P, Bacchiocchi A, McCusker JP, Cheng E, Davis MJ, Goh G, Choi M, et al. Exome sequencing identifies recurrent somatic RAC1 mutations in melanoma. Nature genetics. 2012; 44:1006–1014. [PubMed: 22842228]

Kwon Y, Song W, Droujinine IA, Hu Y, Asara JM, Perrimon N. Systemic organ wasting induced by localized expression of the secreted insulin/IGF antagonist ImpL2. Developmental cell. 2015; 33:36–46. [PubMed: 25850671]

Lee JH, Koh H, Kim M, Park J, Lee SY, Lee S, Chung J. JNK pathway mediates apoptotic cell death induced by tumor suppressor LKB1 in Drosophila. Cell death and differentiation. 2006; 13:1110–1122. [PubMed: 16273080]

Ma X, Li W, Yu H, Yang Y, Li M, Xue L, Xu T. Bendless modulates JNK-mediated cell death and migration in Drosophila. Cell death and differentiation. 2014; 21:407–415. [PubMed: 24162658]

Ma X, Xu W, Zhang D, Yang Y, Li W, Xue L. Wallenda regulates JNK-mediated cell death in Drosophila. Cell death & disease. 2015; 6:e1737. [PubMed: 25950467]

Ma X, Yang L, Yang Y, Li M, Li W, Xue L. dUev1a modulates TNF-JNK mediated tumor progression and cell death in Drosophila. Developmental biology. 2013; 380:211–221. [PubMed: 23726905]

Menendez J, Perez-Garijo A, Calleja M, Morata G. A tumor-suppressing mechanism in Drosophila involving cell competition and the Hippo pathway. Proceedings of the National Academy of Sciences of the United States of America. 2010; 107:14651–14656. [PubMed: 20679206]

Moreno E, Yan M, Basler K. Evolution of TNF signaling mechanisms: JNK-dependent apoptosis triggered by Eiger, the Drosophila homolog of the TNF superfamily. Current biology: CB. 2002; 12:1263–1268. [PubMed: 12176339]

Pagliarini RA, Xu T. A genetic screen in Drosophila for metastatic behavior. Science. 2003; 302:1227–1231. [PubMed: 14551319]

Pastor-Pareja JC, Xu T. Dissecting social cell biology and tumors using Drosophila genetics. Annual review of genetics. 2013; 47:51–74.

Reiter LT, Potocki L, Chien S, Gribskov M, Bier E. A systematic analysis of human disease-associated gene sequences in Drosophila melanogaster. Genome research. 2001; 11:1114–1125. [PubMed: 11381037]

Rudrapatna VA, Cagan RL, Das TK. Drosophila cancer models. Dev Dyn. 2012; 241:107–118. [PubMed: 22038952]

Ryan MB, Der CJ, Wang-Gillam A, Cox AD. Targeting RAS-mutant cancers: is ERK the key? Trends in cancer. 2015; 1:183–198. [PubMed: 26858988]

Samatar AA, Poulikakos PI. Targeting RAS-ERK signalling in cancer: promises and challenges. Nature reviews Drug discovery. 2014; 13:928–942. [PubMed: 25435214]

Srivastava A, Pastor-Pareja JC, Igaki T, Pagliarini R, Xu T. Basement membrane remodeling is essential for Drosophila disc eversion and tumor invasion. Proc Natl Acad Sci U S A. 2007; 104:2721–2726. [PubMed: 17301221]

Stefansson B, Brautigan DL. Protein phosphatase PP6 N terminal domain restricts G1 to S phase progression in human cancer cells. Cell cycle. 2007; 6:1386–1392. [PubMed: 17568194]

Stephen AG, Esposito D, Bagni RK, McCormick F. Dragging ras back in the ring. Cancer cell. 2014; 25:272–281. [PubMed: 24651010]

Uhlirova M, Bohmann D. JNK- and Fos-regulated Mmp1 expression cooperates with Ras to induce invasive tumors in Drosophila. The EMBO journal. 2006; 25:5294–5304. [PubMed: 17082773]

Vidal M, Larson DE, Cagan RL. Csk-deficient boundary cells are eliminated from normal Drosophila epithelia by exclusion, migration, and apoptosis. Developmental cell. 2006; 10:33–44. [PubMed: 16399076]

Vogelstein B, Papadopoulos N, Velculescu VE, Zhou S, Diaz LA Jr, Kinzler KW. Cancer genome landscapes. Science. 2013; 339:1546–1558. [PubMed: 23539594]

Willoughby LF, Schlosser T, Manning SA, Parisot JP, Street IP, Richardson HE, Humbert PO, Brumby AM. An in vivo large-scale chemical screening platform using Drosophila for anti-cancer drug discovery. Disease models & mechanisms. 2013; 6:521–529. [PubMed: 22996645]

Xue L, Igaki T, Kuranaga E, Kanda H, Miura M, Xu T. Tumor suppressor CYLD regulates JNK-induced cell death in Drosophila. Developmental cell. 2007; 13:446–454. [PubMed: 17765686]

Zeng K, Bastos RN, Barr FA, Gruneberg U. Protein phosphatase 6 regulates mitotic spindle formation by controlling the T-loop phosphorylation state of Aurora A bound to its activator TPX2. The Journal of cell biology. 2010; 191:1315–1332. [PubMed: 21187329]

Highlights

- An EMS-based genetic screen in fly identifies Fmt as a tumor suppressor
- Loss of Fmt synergizes with Ras^{V12} to induce JNK-dependent tumorigenesis
- PpV depletion phenocopies Fmt disruption-induced tumorigenesis
- Fmt synergizes with PpV *in vivo*

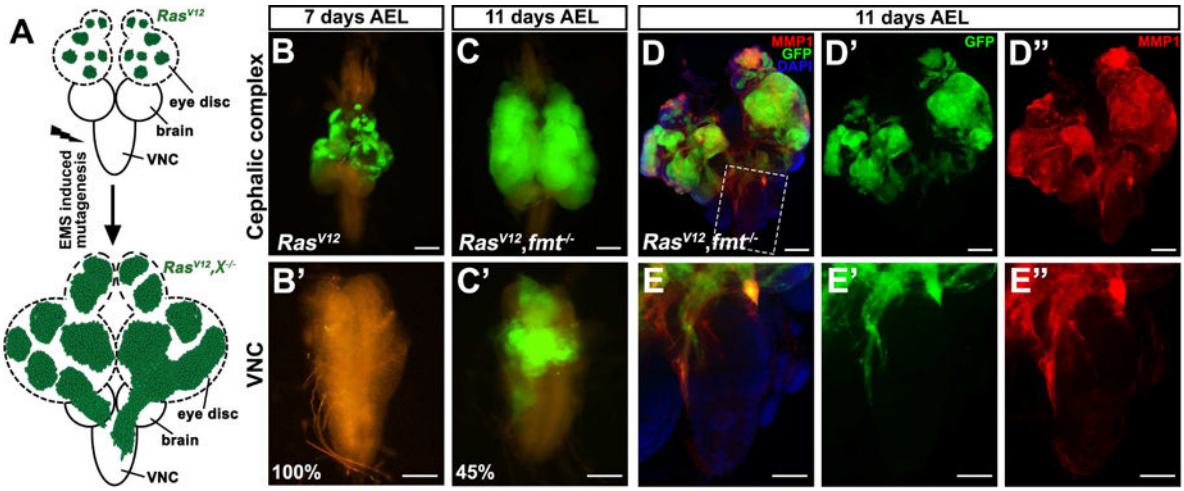

Figure 1. Loss of Fmt synergizes with *Ras*^{V12} to induce tumorigenesis and invasion

(A) Strategy of an EMS-induced forward genetic screen to identify novel *Ras*^{V12} collaborating tumor suppressors on chromosome 3L.

(B–E) Fluorescence micrographs of GFP-labeled clones of dissected eye-antennal disc and ventral nerve cord (VNC) are shown. 7 days after egg laying (AEL), ectopic *Ras*^{V12} expression caused benign tumor growth (B), but not invasion (B′). 11 days AEL, *Ras*^{V12}/*Fmt*$^{-/-}$ tumor bearing animals showed massive growth and invasion into the VNC (C and C′), as indicated by intensive MMP1 staining in both eye disc (D–D″) and VNC (E–E″). Scale bars, 200 μm in (B, C, D–D″), 100 μm in (B′, C′, E–E″). Genotypes: (B) *ey-Flp1*/+; *Act>y*$^{+}$>Gal4, *UAS*-GFP/*UAS-Ras*^{V12}; *tub*-Gal80, FRT79E/FRT79E (C–D) *ey-Flp1*/+; *Act>y*$^{+}$>Gal4, *UAS*-GFP/*UAS-Ras*^{V12}; *tub*-Gal80, FRT79E/*fmt*^{1}, FRT79E. See also Figure S1.

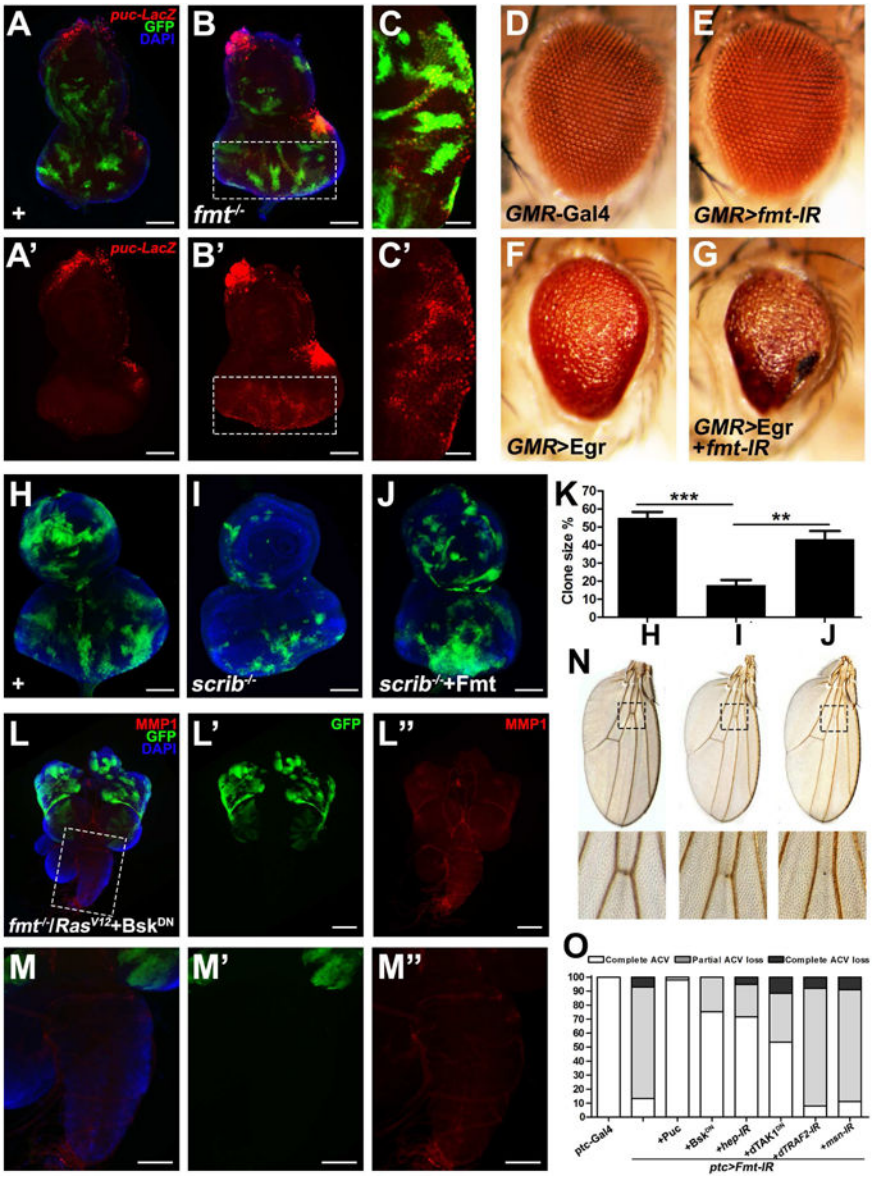

Figure 2. Fmt negatively regulates JNK signaling

(A–C) Fluorescence micrographs of eye discs are shown. Compared with wild type (A), loss of *Fmt* induces mild JNK activation (B and C). (D–G) Light micrographs of *Drosophila* adult eyes of indicated genotypes are shown. Loss of *Fmt* synergistically enhanced *GMR*>Egr-induced small eye phenotype (F and G), whereas expression of *Fmt-IR* alone gave no obvious phenotype (E). (H–K) Compared with wild type (H), *scrib* depletion induced cell elimination (I) was rescued by expression of Fmt (J). (K) Quantification of cell elimination phenotype in H–J. $^{**}P<0.01$, $^{***}P<0.001$. (mean + *s.d.*, n=5). (L–M) Inhibition of JNK signaling completely abolished $Ras^{V12}/Fmt^{-/-}$ induced MMP1 activation and invasion behavior. (N) Light micrographs of *Drosophila* adult wings are shown. Loss of *Fmt* under *ptc*-Gal4 caused partial (middle lane) or complete loss of anterior cross vein (right lane). (O) Quantification of vein loss phenotype of indicated genotypes. Scale bars, 100 μm in (A, B, H–J, M–M″), 50 μm in (C, C′), 200 μm in (L–L″). Genotypes: (A) *ey-Flp1*/+;

Act>y^{+}>Gal4, *UAS*-GFP/*+*; *tub*-Gal80, FRT79E, *puc*^{E69}/FRT79E (B–C) *ey-Flp1*/+; *Act>y*$^{+}$>Gal4, *UAS*-GFP/+; *tub*-Gal80, FRT79E, *puc*^{E69}/*fmt*^{1}, FRT79E (D) *GMR*-Gal4/+ (E) *GMR*-Gal4/+; *UAS-Fmt-IR*/+ (F) *UAS*-Egr/+; *GMR*-Gal4/+ (G) *UAS*-Egr/*UAS-Fmt-IR*; *GMR*-Gal4/+ (H) *eyFlp1/+*; *Act>y*$^{+}$>Gal4, *UAS*-GFP.S65T/+; FRT82B, *tub*-Gal80/FRT82B (I) *eyFlp1/+*; *Act>y*$^{+}$>Gal4, *UAS*-GFP.S65T/+; FRT82B, *tub*-Gal80/FRT82B, *scrib*^{1} (J) *eyFlp1/+*; *Act>y*$^{+}$>Gal4, *UAS*-GFP.S65T/*UAS*-Fmt; FRT82B, *tub*-Gal80/FRT82B, *scrib*^{1} (L–M) *ey-Flp1*/*UAS*-Bsk^{DN}; *Act>y*$^{+}$>Gal4, *UAS*-GFP/*UAS-Ras*^{V12}; *tub*-Gal80, FRT79E/*fmt*^{1}, FRT79E (O) Left to right, *ptc*-Gal4, *UAS*-GFP/+. *ptc*-Gal4, *UAS*-GFP/*UAS-Fmt-IR*. *ptc*-Gal4, *UAS*-GFP/*UAS-Fmt-IR*; *UAS*-Puc/+. *ptc*-Gal4, *UAS*-GFP/*UAS-Fmt-IR*; *UAS*-Bsk^{DN}/+. *ptc*-Gal4, *UAS*-GFP/*UAS-Fmt-IR*; *UAS-hep-IR*/+. *ptc*-Gal4, *UAS*-GFP/*UAS-Fmt-IR*; *UAS*-dTAK1^{DN}/+. *ptc*-Gal4, *UAS*-GFP/*UAS-Fmt-IR*; *UAS-dTRAF2-IR*/+. *ptc*-Gal4, *UAS*-GFP/*UAS-Fmt-IR*; *UAS-msn-IR*/+. See also Figure S2.

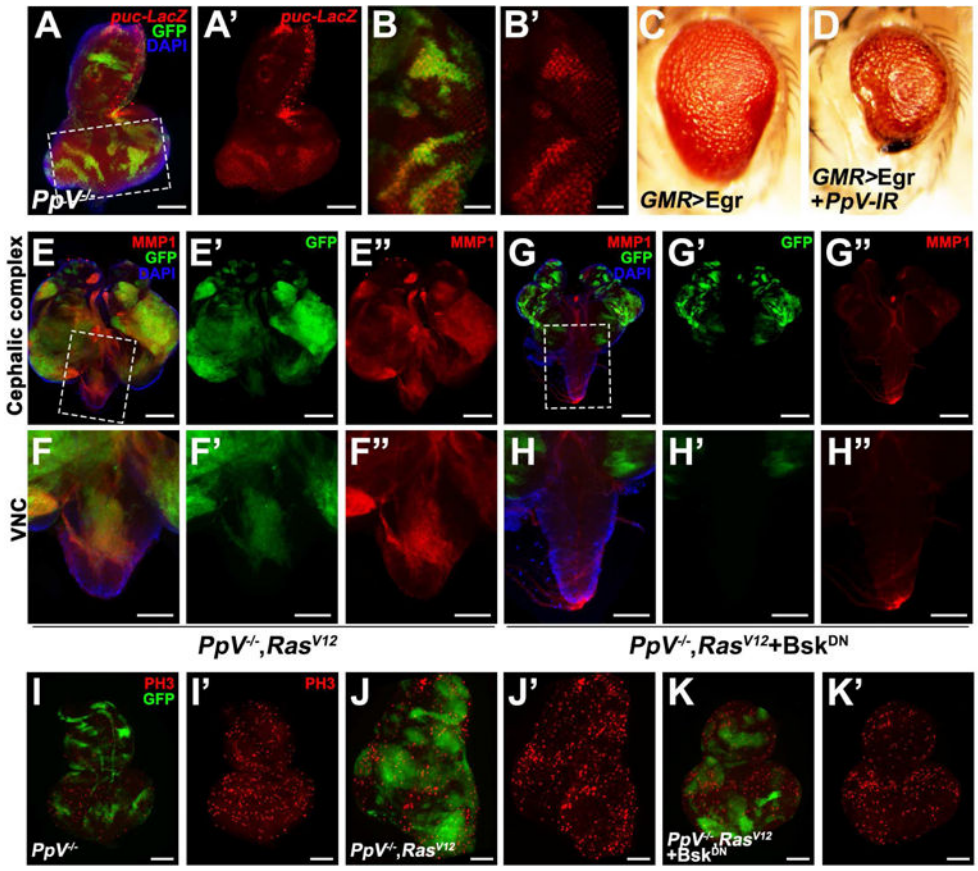

Figure 3. Loss of *PpV* collaborates with Ras^{V12} to drive JNK-dependent tumor growth and invasion

(A–B) Loss of *PpV* induces mild JNK activation. (C–D) Light micrographs of *Drosophila* adult eyes of indicated genotypes are shown. Loss of *PpV* synergistically enhances *GMR*>Egr induced small eye. (E–H) Fluorescence micrographs of GFP-labeled clones of eye-antennal disc and VNC are shown. $PpV^{-/-}/Ras^{V12}$ induced MMP1 activation, tumorigenesis and invasion behavior (E and F) were all completely suppressed by blocking JNK signaling (G and H). (I–K) Compared with loss of *PpV* alone (I′), $PpV^{-/-}/Ras^{V12}$ clones displayed strongly increased mitosis (J′), which was dramatically suppressed by reducing JNK activity (K′). Scale bars, 100 μm in (A, F–F″, H–H″, I–K′), 50 μm in (B–B′), 200 μm in (E–E″, G–G″). Genotypes: (A–B) $PpV^{\Delta 1}$, FRT19A/*tub*-Gal80, FRT19A; *ey-Flp5*, *Act*>y^{+}>Gal4, *UAS*-GFP/+; puc^{E69}/+ (C) *UAS*-Egr/+; *GMR*-Gal4/+ (D) *UAS*-Egr/+; *GMR*-Gal4/*UAS-PpV-IR* (E, F, J) $PpV^{\Delta 1}$, FRT19A/*tub*-Gal80, FRT19A; *ey-Flp5*, *Act*>y^{+}>Gal4, *UAS*-GFP/$UAS\text{-}Ras^{V12}$ (G, H, K) $PpV^{\Delta 1}$, FRT19A/*tub*-Gal80, FRT19A; *ey-Flp5*, *Act*>y^{+}>Gal4, *UAS*-GFP/$UAS\text{-}Ras^{V12}$; *UAS*-Bsk^{DN}/+ (I) $PpV^{\Delta 1}$, FRT19A/*tub*-Gal80, FRT19A; *ey-Flp5*, *Act*>y^{+}>Gal4, *UAS*-GFP/+. See also Figure S3.

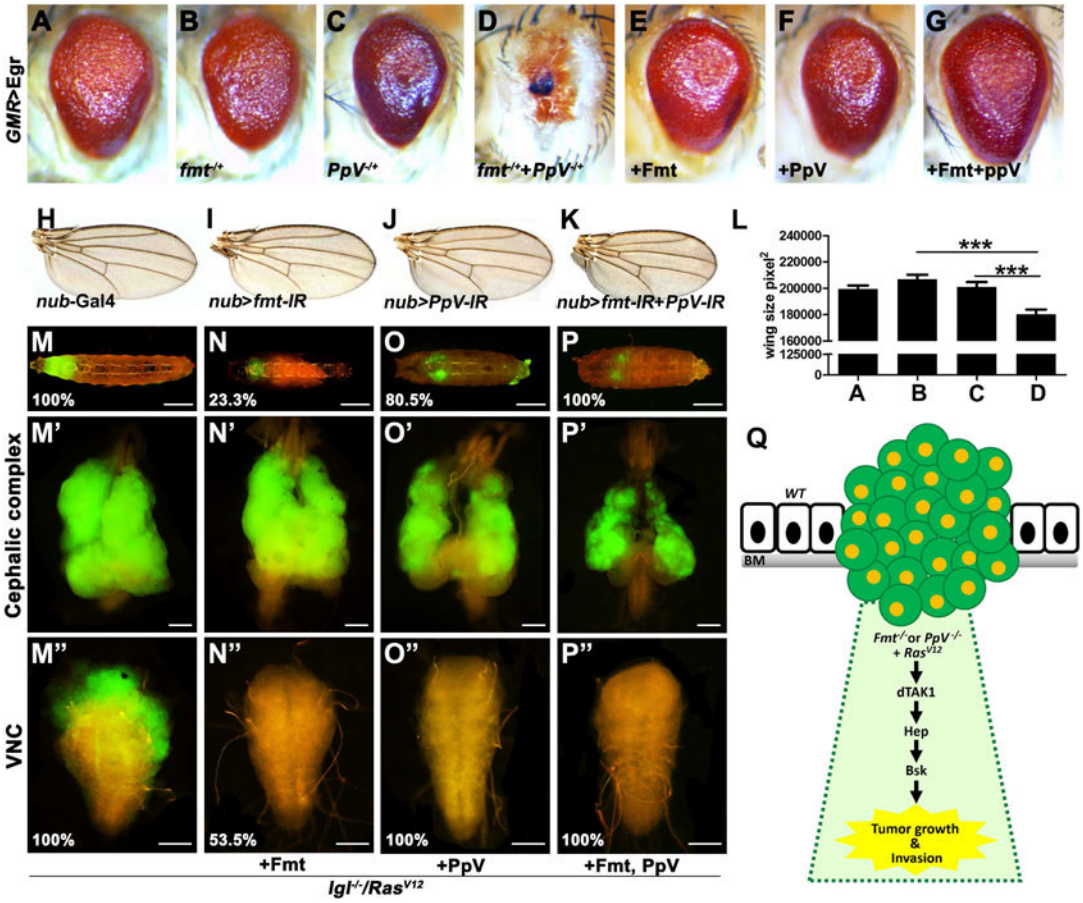

Figure 4. PpV synergizes with Fmt *in vivo*

(A–G) Light micrographs of *Drosophila* adult eyes are shown. Removing one copy of *fmt* or *PpV* slightly enhances *GMR*>Egr small eye, while simultaneously remove one copy of each results in complete eye loss. Co-expression of Fmt and PpV synergistically suppress *GMR*>Egr eye phenotype.

(H–K) Light micrographs of *Drosophila* adult wings are shown. Compared with controls (H), loss of either *Fmt* (I) or *PpV* (J) driven by *nub*-Gal4 produced no obvious phenotype, while co-expression of *Fmt-IR* and *PpV-IR* resulted in smaller wings (K). (L) Quantification data of wing size in A–D. (M–P) Fluorescence micrographs of GFP-labeled clones of eye-antennal disc and VNC are shown. $lgl^{-/-}/Ras^{V12}$ induced tumor overgrowth (M′), invasion (M″), and eventually death as giant larvae (M). Ectopic expression of Fmt partially restored the pupation (N), significantly suppressed tumor invasion (N″), but not tumor growth (N′). Expression of PpV alone is sufficient to completely suppressed invasive phenotype (O″) and dramatically restored pupation (O), whereas tumor size was only slightly suppressed, if there is any (O′). Co-expression of Fmt and PpV dramatically suppressed tumor progression, including tumorigenesis and invasion (P′ and P″), and rescued all the animals to pupal stage (P). % indicates phenotype penetrance ratio. (Q) Model of PpV and Fmt in Ras^{V12}-induced tumorigenesis. Scale bars, 400 μm in (M–P), 200 μm in (M′–P′), 100 μm in (M″–P″). Genotypes: (A) *UAS*-Egr/+; *GMR*-Gal4/+ (B) *UAS*-Egr/+; *GMR*-Gal4/fmt^{1}, FRT79E (C) $PpV^{\Delta 1}$, FRT19A/+; *UAS*-Egr/+; *GMR*-Gal4/+ (D) $PpV^{\Delta 1}$, FRT19A/+; *UAS*-Egr/+; *GMR*-

Gal4/*fmt*^{1}, FRT79E (E) *UAS*-Egr/*UAS*-Fmt; *GMR*-Gal4/+ (F) *UAS*-Egr/+; *GMR*-Gal4/*UAS*-PpV (G) *UAS*-Egr/*UAS*-Fmt; *GMR*-Gal4/*UAS*-PpV (H) *nub*-Gal4/+ (I) *nub*-Gal4/*UAS-Fmt-IR* (J) *nub*-Gal4/+; *UAS-PpV-IR*/+ (K) *nub*-Gal4/*UAS-Fmt-IR*; *UAS-PpV-IR*/+ (M) *ey-Flp1*/+; *tub*-Gal80, FRT40A/*lgl*^{4}, FRT40A, *UAS-Ras*^{V12}; *Act>y*$^{+}$>Gal4, *UAS*-GFP/+ (N) *ey-Flp1*/+; *tub*-Gal80, FRT40A/*lgl*^{4}, FRT40A, *UAS-Ras*^{V12}; *Act>y*$^{+}$>Gal4, *UAS*-GFP/*UAS*-Fmt (O) *ey-Flp1*/+; *tub*-Gal80, FRT40A/*lgl*^{4}, FRT40A, *UAS-Ras*^{V12}; *Act>y*$^{+}$>Gal4, *UAS*-GFP/*UAS*-PpV (P) *ey-Flp1*/+; *tub*-Gal80, FRT40A/*lgl*^{4}, FRT40A, *UAS-Ras*^{V12}; *Act>y*$^{+}$>Gal4, *UAS*-GFP/*UAS*-Fmt, *UAS*-PpV. See also Figure S4.